

# Branching Fractions for Transitions of $\psi(2S)$ to $J/\psi$

H. Mendez,<sup>1</sup> J. Y. Ge,<sup>2</sup> D. H. Miller,<sup>2</sup> I. P. J. Shipsey,<sup>2</sup> B. Xin,<sup>2</sup> G. S. Adams,<sup>3</sup> M. Anderson,<sup>3</sup> J. P. Cummings,<sup>3</sup> I. Danko,<sup>3</sup> D. Hu,<sup>3</sup> B. Moziak,<sup>3</sup> J. Napolitano,<sup>3</sup> Q. He,<sup>4</sup> J. Insler,<sup>4</sup> H. Muramatsu,<sup>4</sup> C. S. Park,<sup>4</sup> E. H. Thorndike,<sup>4</sup> F. Yang,<sup>4</sup> M. Artuso,<sup>5</sup> S. Blusk,<sup>5</sup> S. Khalil,<sup>5</sup> J. Li,<sup>5</sup> R. Mountain,<sup>5</sup> S. Nisar,<sup>5</sup> K. Randrianarivony,<sup>5</sup> N. Sultana,<sup>5</sup> T. Skwarnicki,<sup>5</sup> S. Stone,<sup>5</sup> J. C. Wang,<sup>5</sup> L. M. Zhang,<sup>5</sup> G. Bonvicini,<sup>6</sup> D. Cinabro,<sup>6</sup> M. Dubrovin,<sup>6</sup> A. Lincoln,<sup>6</sup> P. Naik,<sup>7</sup> J. Rademacker,<sup>7</sup> D. M. Asner,<sup>8</sup> K. W. Edwards,<sup>8</sup> J. Reed,<sup>8</sup> R. A. Briere,<sup>9</sup> T. Ferguson,<sup>9</sup> G. Tatishvili,<sup>9</sup> H. Vogel,<sup>9</sup> M. E. Watkins,<sup>9</sup> J. L. Rosner,<sup>10</sup> J. P. Alexander,<sup>11</sup> D. G. Cassel,<sup>11</sup> J. E. Duboscq,<sup>11</sup> R. Ehrlich,<sup>11</sup> L. Fields,<sup>11</sup> L. Gibbons,<sup>11</sup> R. Gray,<sup>11</sup> S. W. Gray,<sup>11</sup> D. L. Hartill,<sup>11</sup> B. K. Heltsley,<sup>11</sup> D. Hertz,<sup>11</sup> J. M. Hunt,<sup>11</sup> J. Kandaswamy,<sup>11</sup> D. L. Kreinick,<sup>11</sup> V. E. Kuznetsov,<sup>11</sup> J. Ledoux,<sup>11</sup> H. Mahlke-Krüger,<sup>11</sup> D. Mohapatra,<sup>11</sup> P. U. E. Onyisi,<sup>11</sup> J. R. Patterson,<sup>11</sup> D. Peterson,<sup>11</sup> D. Riley,<sup>11</sup> A. Ryd,<sup>11</sup> A. J. Sadoff,<sup>11</sup> X. Shi,<sup>11</sup> S. Stroiney,<sup>11</sup> W. M. Sun,<sup>11</sup> T. Wilksen,<sup>11</sup> S. B. Athar,<sup>12</sup> R. Patel,<sup>12</sup> J. Yelton,<sup>12</sup> P. Rubin,<sup>13</sup> B. I. Eisenstein,<sup>14</sup> I. Karliner,<sup>14</sup> S. Mehrabyan,<sup>14</sup> N. Lowrey,<sup>14</sup> M. Selen,<sup>14</sup> E. J. White,<sup>14</sup> J. Wiss,<sup>14</sup> R. E. Mitchell,<sup>15</sup> M. R. Shepherd,<sup>15</sup> D. Besson,<sup>16</sup> T. K. Pedlar,<sup>17</sup> D. Cronin-Hennessy,<sup>18</sup> K. Y. Gao,<sup>18</sup> J. Hietala,<sup>18</sup> Y. Kubota,<sup>18</sup> T. Klein,<sup>18</sup> B. W. Lang,<sup>18</sup> R. Poling,<sup>18</sup> A. W. Scott,<sup>18</sup> P. Zweber,<sup>18</sup> S. Dobbs,<sup>19</sup> Z. Metreveli,<sup>19</sup> K. K. Seth,<sup>19</sup> A. Tomaradze,<sup>19</sup> J. Libby,<sup>20</sup> A. Powell,<sup>20</sup> G. Wilkinson,<sup>20</sup> K. M. Ecklund,<sup>21</sup> W. Love,<sup>22</sup> and V. Savinov<sup>22</sup>

(CLEO Collaboration)

<sup>1</sup>*University of Puerto Rico, Mayaguez, Puerto Rico 00681*

<sup>2</sup>*Purdue University, West Lafayette, Indiana 47907, USA*

<sup>3</sup>*Rensselaer Polytechnic Institute, Troy, New York 12180, USA*

<sup>4</sup>*University of Rochester, Rochester, New York 14627, USA*

<sup>5</sup>*Syracuse University, Syracuse, New York 13244, USA*

<sup>6</sup>*Wayne State University, Detroit, Michigan 48202, USA*

<sup>7</sup>*University of Bristol, Bristol BS8 1TL, UK*

<sup>8</sup>*Carleton University, Ottawa, Ontario, Canada K1S 5B6*

<sup>9</sup>*Carnegie Mellon University, Pittsburgh, Pennsylvania 15213, USA*

<sup>10</sup>*Enrico Fermi Institute, University of Chicago, Chicago, Illinois 60637, USA*

<sup>11</sup>*Cornell University, Ithaca, New York 14853, USA*

<sup>12</sup>*University of Florida, Gainesville, Florida 32611, USA*

<sup>13</sup>*George Mason University, Fairfax, Virginia 22030, USA*

<sup>14</sup>*University of Illinois, Urbana-Champaign, Illinois 61801, USA*

<sup>15</sup>*Indiana University, Bloomington, Indiana 47405, USA*

<sup>16</sup>*University of Kansas, Lawrence, Kansas 66045, USA*

<sup>17</sup>*Luther College, Decorah, Iowa 52101, USA*

<sup>18</sup>*University of Minnesota, Minneapolis, Minnesota 55455, USA*

<sup>19</sup>*Northwestern University, Evanston, Illinois 60208, USA*

<sup>20</sup>*University of Oxford, Oxford OX1 3RH, UK*

<sup>21</sup>*State University of New York at Buffalo, Buffalo, New York 14260, USA*

<sup>22</sup>*University of Pittsburgh, Pittsburgh, Pennsylvania 15260, USA*

(Dated: April 28, 2008)

## Abstract

We report determination of branching fractions for the decays  $\psi(2S) \rightarrow h + J/\psi$ , where  $h = \text{any}$ ,  $\pi^+ \pi^-$ ,  $\pi^0 \pi^0$ ,  $\eta$ ,  $\pi^0$ , and  $\gamma\gamma$  through  $\chi_{c0,1,2}$ . These measurements use 27M  $\psi(2S)$  decays produced in  $e^+ e^-$  collision data collected with the CLEO detector. The resulting branching fractions and ratios thereof improve upon previously achieved precision in all cases, and in combination with other measurements permit determination of  $\mathcal{B}(\chi_{cJ} \rightarrow \gamma J/\psi)$  and  $\mathcal{B}(\psi(2S) \rightarrow \text{light hadrons})$ .

The study of charmonium has entered an era in which many of the broad features are finally known, increasingly focusing attention upon the details of both production and decay [1]. The decays of  $\psi(2S)$  in particular have become very well studied. About 4/5 of all  $\psi(2S)$  decays are through de-excitation, mostly by hadronic transition to the  $J/\psi$ , but also through radiative decay to the  $\chi_{cJ}$  states. Measurements of rates for such processes enable meaningful comparison with theory and extrapolation to similar mechanisms in the  $\Upsilon$  system. The listed transitions can be used to isolate and study lower-lying  $c\bar{c}$  states. For example, the decay  $\psi(2S) \rightarrow \pi^+\pi^-J/\psi$  is useful because this is the most common and the most accessible experimentally; inclusive and exclusive  $J/\psi$  decays are often identified by tagging the recoil dipion. The corresponding  $\psi(2S)$  decay rate is therefore a target for continuing precision improvements. Similarly,  $\chi_{cJ}$  mesons can often be tagged for study by the transition photons. The *inclusive* rate for transitions to the  $J/\psi$  is also a crucial input to predictions for  $c\bar{c}$  annihilation rates because it limits the remainder. Hence refining the rates for  $\psi(2S)$ -to- $J/\psi$  transitions remains an experimental priority. The first comprehensive look at all transitions simultaneously by a single experiment was reported by CLEO [2] in 2005; absolute measurements were limited by a 3% uncertainty in the number of  $\psi(2S)$  produced, and many ratios of rates were limited by statistics. Further investigations with a larger dataset and improved systematic uncertainties are certainly warranted.

This article describes a measurement of ratios of branching fractions  $\psi(2S) \rightarrow h + J/\psi$ , where  $h = \pi^+\pi^-, \pi^0\pi^0, \eta(\rightarrow \gamma\gamma, \pi^+\pi^-\pi^0), \pi^0, \gamma\gamma$  through  $\gamma\chi_{cJ}$  (for which process we will also use the expression  $\gamma(\gamma J/\psi)_{\chi_{cJ}}$ ), and the inclusive branching fraction  $\mathcal{B}(\psi(2S) \rightarrow \text{any} + J/\psi)$ , in which only the  $J/\psi$  is identified. We separately determine  $\mathcal{B}_{+-} = \mathcal{B}(\psi(2S) \rightarrow \pi^+\pi^-J/\psi)$  with the  $J/\psi$  decaying inclusively, which we denote by  $J/\psi \rightarrow X$ .

We use  $e^+e^-$  collision data at and below the  $\psi(2S)$  resonance,  $E_{\text{cm}} = 3.686 \text{ GeV}$  ( $\int \mathcal{L} dt = 53.8 \text{ pb}^{-1}$ , corresponding to 27M  $\psi(2S)$  decays) and  $E_{\text{cm}} = 3.670 \text{ GeV}$  (“continuum” data,  $\int \mathcal{L} dt = 20.6 \text{ pb}^{-1}$ ). Events were acquired at the Cornell Electron Storage Ring (CESR) [3] with the CLEO detector [4], mostly in the CLEO-c configuration (95%), with the balance from CLEO III. The detector features a solid angle coverage of 93% for charged and neutral particles. The charged particle tracking system operates in a 1.0 T magnetic field along the beam axis and achieves a momentum resolution of  $\sim 0.6\%$  at momenta of  $1 \text{ GeV}/c$ . The CsI crystal calorimeter attains photon energy resolutions of 2.2% for  $E_\gamma = 1 \text{ GeV}$  and 5% at 100 MeV.

For the measurement of branching fractions relative to one another, the  $J/\psi$  is identified through its decay to  $\mu^+\mu^-$  or  $e^+e^-$ . We require  $|\cos\theta_{\text{trk}}| < 0.83$  for both lepton tracks, where the polar angle  $\theta$  is measured with respect to the positron direction of incidence. The ratios of calorimeter shower energy to track momentum,  $E/p$ , for the lepton candidates, taken to be the two tracks of highest momentum in the event, must be larger than 0.85 for one electron and above 0.5 for the other, or in the case of muons smaller than 0.25 for one and below 0.5 for the other. In order to salvage lepton pairs that have radiated photons and would hence lose too much energy to remain identifiable as a  $J/\psi$ , we add bremsstrahlung photon candidates found within a cone of 100 mrad to the three-vector of each lepton track at the interaction point (IP). The  $J/\psi$  candidate is retained only if constrained fits to the two tracks and bremsstrahlung candidates to a common vertex and to the mass of the  $J/\psi$  fulfill  $\chi^2_{\text{V}}/\text{d.o.f.} < 20$  and  $\chi^2_{\text{M}}/\text{d.o.f.} < 20$ , respectively. The  $\chi^2_{\text{M}}/\text{d.o.f.}$  restriction corresponds roughly to demanding that the dilepton mass lie between 3.03 and 3.16 GeV.

For  $\psi(2S) \rightarrow \text{any} + J/\psi$ , cosmic ray background is rejected based on the distance of the track impact parameters to the event interaction point ( $< 2 \text{ mm}$ ), and on the  $J/\psi$  momentum

$(p_{J/\psi} > 50 \text{ MeV}/c)$ . To suppress background from continuum reactions we require  $p_{J/\psi} < 570 \text{ MeV}$ . Radiative lepton pair production and radiative returns to the  $J/\psi$  ( $e^+e^- \rightarrow \gamma J/\psi$ ) are suppressed by requiring  $|\cos \theta_{J/\psi}| < 0.98$  and for the dielectron mode by demanding  $\cos \theta_{e^+} < 0.5$ . Decays of  $\psi(2S)$  to final states not involving a  $J/\psi$  can contaminate the any +  $J/\psi$  mode if two oppositely charged particles satisfy the lepton identification and kinematic criteria. Monte Carlo (MC) studies indicate such backgrounds are very small, leading to no background subtraction and an assignment of a systematic uncertainty in rate of 0.2% ( $\mu^+\mu^-$ ) and 0.1% ( $e^+e^-$ ).

For  $\pi^+\pi^-J/\psi$  [ $\pi^0\pi^0J/\psi$ ] we demand the presence of two oppositely charged tracks [two  $\pi^0$  candidates]. In both cases, the mass recoiling against the dipion is required to be 3.05-3.15 GeV. To suppress background from radiative Bhabha and dimuon pairs, where the photon converts and the resulting tracks are associated with the  $\pi^+\pi^-$ , we require  $m(\pi^+\pi^-) > 0.35 \text{ MeV}$ .

Any photon candidate reconstructed in any of the exclusive modes must lie in the central region of the calorimeter ( $|\cos \theta_\gamma| < 0.75$ ) and be isolated (not aligned with the initial momentum of a track within 100 mrad and not closer than 30 cm to a shower that is matched to a track). We impose mode-dependent requirements on the photon energies,  $E_\gamma$ .

All  $\pi^0$  candidates are formed using two photon showers, each of at least 30 MeV in energy, that together have an invariant mass of 100-160 MeV. For  $\pi^0\pi^0J/\psi$  and  $(\pi^+\pi^-\pi^0)_\eta J/\psi$ , but not for  $\pi^0J/\psi$ , we constrain their four-momentum to the  $\pi^0$  mass. For  $\pi^0J/\psi$ , the softer of the two photons cannot lie within  $E_\gamma = 100\text{-}200 \text{ MeV}$  in order to suppress background from  $\gamma\chi_{cJ}$  decays.

To select  $(\pi^+\pi^-\pi^0)_\eta$  events, we require two oppositely-charged tracks and a  $\pi^0$  candidate, which together have an invariant mass of 535-560 MeV. For  $(\gamma\gamma)_\eta J/\psi$ , we require that both photons have  $E_\gamma > 200 \text{ MeV}$  and  $m(\gamma\gamma) = 500\text{-}600 \text{ MeV}$ . Leakage of the high-rate process  $\pi^0\pi^0J/\psi$  into the other modes with only two photons and no tracks is suppressed by requiring that for  $\pi^0J/\psi$  and  $\gamma\chi_{cJ}$  the third-largest shower energy in the event does not exceed 50 MeV. Both  $\eta$  decay modes are combined into a common  $\eta$  measurement using their branching fractions [5].

For  $\pi^0J/\psi$  [ $\eta J/\psi$ ], we only keep events where  $J/\psi$  candidates have a momentum within 490-570 MeV/ $c$  [170-230] MeV/ $c$ .

For  $\gamma(\gamma J/\psi)_{\chi_{cJ}}$ , we tally yields, cross-feeds, and backgrounds separately for the following windows applicable to  $E_{\gamma\text{-low}}$ , the lower photon energy of the two: 90-145 MeV ( $\chi_{c2}$ ), 145-200 ( $\chi_{c1}$ ), 200-245 (between  $\chi_{c1}$  and  $\chi_{c0}$ ), and 245-290 ( $\chi_{c0}$ ). For the last two categories, we subject the event to a final kinematic fit constraining the  $J/\psi$  and the two photons to the  $\psi(2S)$  four-momentum. The  $J/\psi$  momentum must lie in the range 250-500 MeV to eliminate  $\pi^0J/\psi$  and  $(\gamma\gamma)_\eta J/\psi$  cross-feed, and for  $J = 1, 2$ , the invariant mass recoiling against the two photons must lie near the  $J/\psi$  mass, 3.05-3.13 GeV.

After these requirements, the event samples are clean. This is demonstrated for any +  $J/\psi$ ,  $\pi^+\pi^-J/\psi$  and  $\pi^0\pi^0J/\psi$ , as well as  $\eta J/\psi$  and  $\pi^0J/\psi$  in Figs. 1, 2, and 3. The remaining background is readily estimated and subtracted. The most important backgrounds come from cross-feed among our signal modes, for which we account using the measured yield from our sample as background normalization. We also calculate background from  $\eta J/\psi$  with  $\eta$  decaying other than to  $\gamma\gamma$  and  $\pi^+\pi^-\pi^0$ , normalizing with branching fractions determined elsewhere [5]. We subtract background from continuum by counting the yield observed in our continuum data, scaled by luminosity and the  $1/s$  dependence of the cross-sections. The yields are listed in Table I.

We determine the detection efficiency for all modes we study using signal Monte Carlo (MC) samples generated with EVTGEN [6], including photon production in the decay of the  $J/\psi$  (“decay radiation”) [7], and a GEANT-based [8] detector simulation. The  $\pi\pi J/\psi$  samples were produced using the EVTGEN model VVPIPI, with a slight reweighting of the dipion mass distribution to better represent the measured spectrum [2]. Allowing for a relative  $D$ -wave component in the dipion system of the strength found in Ref. [9] changes the efficiency by at most 0.1% (relative). The angular distributions for the  $\chi_{cJ}$  decays were generated according to the formalism presented in Ref. [10]. In addition, for the  $(\gamma\gamma)_{\chi_{cJ}}$  modes, we simulated the  $\chi_{cJ}$  line shape as Breit-Wigner distributions out to 20/228/19 ( $J = 0/1/2$ ) times the full width, using masses and widths from Ref. [11], and scaled by  $E_{\gamma\text{-low}}^3$  as appropriate for E1 transitions [12]. We compute the efficiency for any  $+ J/\psi$  from the weighted sum of the individual signal MC samples, where the weight is the relative occurrence as measured in our data. We will show later that the sum of our exclusive channels describes the population observed in the inclusive selection adequately.

The following contributions to the uncertainty were evaluated: MC statistics (at the level of 1%), tracking (0.3% per track, added linearly), photon detection (0.4% per photon, added linearly), MC modeling (about 1%, additionally 2% for the two-photon recoil restriction for the  $\chi_{cJ}$  modes) trigger (0.1-0.4%, depending on decay mode), uncertainty of the background subtraction (stemming from all statistical uncertainties involved).

The  $\chi_{c0}$  background merits some discussion. The signal rate is heavily affected by the understanding of the area between the  $\chi_{c1}$  and  $\chi_{c0}$ , since whatever populates this region also feeds into the  $\chi_{c0}$  window. We noted in our 2005 analysis [2] an excess of unexplained events in  $E_{\gamma\text{-low}} = 200\text{-}245\text{ MeV}$  and confirm a similar production rate here with more data (Fig. 4). However, our simulation of this region has improved in several ways that significantly raise the MC expectation for  $E_{\gamma\text{-low}} = 200\text{-}245\text{ MeV}$ , in particular through the aforementioned  $E_{\gamma\text{-low}}^3$  weighting and through the continuation of the Breit-Wigner distribution from the  $\chi_{c1}$  across this region and extending into that of the  $\chi_{c0}$ . The  $\chi_{c1,2}$  measurements are not affected by these considerations due to their much larger rate (the  $\chi_{c2,1,0}$  raw yields compare roughly as 20:40:1). The events with  $E_{\gamma\text{-low}} = 200\text{-}245\text{ MeV}$  exhibit the expected behavior for  $\gamma\gamma J/\psi$  events and are qualitatively comparable to those in neighboring regions in  $E_{\gamma\text{-low}}$ , namely: the quality of the  $J/\psi$  fit is comparable, there is no indication of missing energy or momentum, and the lateral shower profile for photon candidates is consistent with this assumption.

We have studied several ways to explain the data in the intermediate region as well as the adjacent areas: variation of the  $\chi_{c1}$  width from 0.92 MeV to 1.00 MeV, removal of the  $E_{\gamma}^3$  weighting, allowance for a phase-space-like component where the  $\psi(2S)$  de-excitation takes place through two non-resonant photons (denoted by  $(\gamma\gamma)_{\text{nr}}$ ), and combinations of these. Most of the scenarios can give a satisfactory description with different component weightings, but result in substantial variations of the  $\chi_{c0}$  rate due to the different apportionment of the observed yields to signal and background. Our data do not allow us to distinguish among the possibilities explored, which results in correspondingly large background-related contributions to the systematic uncertainty ( $\chi_{c0}$ : 10%,  $\chi_{c1}$ : 1.0%,  $\chi_{c2}$ : 0.8%). In any of these scenarios, more events in the  $\chi_{c0}$  region are attributed to background than in Ref. [2]. We quote the result obtained with our nominal  $\chi_{c1}$  width, with  $E_{\gamma}^3$  weighting, and with a phase-space-like component  $(\gamma\gamma)_{\text{nr}}$ , as displayed in Fig. 4. Since any sensitivity to the possible additional  $(\gamma\gamma)_{\text{nr}}$  component is restricted to the region between  $\chi_{c0}$  and  $\chi_{c1}$  (and not unambiguous there), we cannot quantify the magnitude of such a contribution any more

precisely than to say that a branching fraction up to  $1 \times 10^{-3}$  is compatible with our data.

Since we measure ratios of yields, many systematic uncertainties cancel, most notably those related to lepton species and  $J/\psi$  fitting. To verify this, we compare ratios measured using  $J/\psi \rightarrow e^+e^-$  with those determined using  $J/\psi \rightarrow \mu^+\mu^-$ . All ratios are close to unity; for the seven ratios involving  $\pi^+\pi^-J/\psi$  we compute  $\chi^2 = 3.0$  for six degrees of freedom.

Table I shows results for the branching fraction ratios, after combining the two measurements from  $J/\psi \rightarrow e^+e^-$  and  $\mu^+\mu^-$ . Adding all ratios of exclusive decays to the inclusive one,  $\Sigma_h[(h + J/\psi)/(any + J/\psi)]$ , leads to a sum that agrees with unity within 0.9% or  $1\sigma$ . This favorable comparison is an indication that the contribution from modes not covered in this analysis (such as  $\gamma\gamma J/\psi$  through  $\eta_c(2S)$ ,  $\pi^+\pi^-\pi^0J/\psi$ , etc.) is small.

We now describe a measurement of the  $\psi(2S) \rightarrow \pi^+\pi^-J/\psi$ ,  $J/\psi \rightarrow X$  production rate. It proceeds identically to the one detailed in Ref. [13], where it was used as the denominator in the determination of  $\mathcal{B}(J/\psi \rightarrow \ell^+\ell^-)$ . The presence of the  $J/\psi$  is inferred through the  $\pi^+\pi^-$  recoil mass spectrum. The pion candidates must consist of two oppositely charged tracks that obey loose quality criteria,  $p_t > 150$  MeV,  $|\cos\theta| < 0.83$ , and  $m(\pi^+\pi^-) > 300$  MeV. The recoil mass spectrum, shown in Fig. 5, is fit with a signal shape using the  $m(\pi^+\pi^-)$ -recoil spectrum from  $\pi^+\pi^-(\ell^+\ell^-)$  data events, selected with the same criteria for the pions as the inclusive  $J/\psi \rightarrow X$  sample (overlaid in Fig. 5), and a second-order polynomial background to extract the yield of  $\pi^+\pi^-(X)_{J/\psi}$  events:  $3.851 \times 10^6$ . The fit has a confidence level of 98.8%. The efficiency determination is potentially hampered by the lack of knowledge of many  $J/\psi$  branching fractions. In practice, however, it is found to be nearly independent of  $J/\psi$  decay mode, although it can be expected to depend weakly upon the track multiplicity, as detailed in Ref. [13]. We therefore use a sample approximating the spectrum in data with a weighted sum of signal MC of various multiplicities, including well-measured decays like  $J/\psi \rightarrow \ell^+\ell^-$ . The agreement between data and the sum of MC predictions thus obtained is good [13]. The detection efficiency determined from the weighted sum of individual efficiencies is found to be 40.16%. Systematic uncertainties stem from uncertainties in the efficiency weights and modeling, translating into 0.7%, sensitivity to the fit range in the signal yield extraction, 0.2%. The result for the number of  $\psi(2S) \rightarrow \pi^+\pi^-J/\psi$  events produced is  $(9.589 \pm 0.020 \pm 0.070) \times 10^6$ .

The number of  $\psi(2S)$  is measured in a manner similar to that described in Ref. [14]. Hadronic event candidates are identified by requiring three tracks ( $N_{\text{trk}} \geq 3$ ) and restrictions on the following quantities: summed energies from tracks and showers,  $E_{\text{vis}}$ , amounting to at least  $0.3E_{\text{cm}}$ , and furthermore for  $N_{\text{trk}} = 3, 4$  a summed energy deposition in the calorimeter of more than  $0.15E_{\text{cm}}$ , and either this sum less than  $0.75E_{\text{cm}}$  or the highest individual shower less than  $0.75E_{\text{beam}}$ . The  $z$ -component of the event vertex,  $z_{\text{vtx}}$ , must be within 5 cm of the beam spot center.

The continuum contamination consists of  $e^+e^- \rightarrow \ell^+\ell^-$  ( $\ell \equiv e$ ,  $\mu$ , or  $\tau$ ), light hadron production through  $e^+e^-$  annihilation or two-photon collisions, radiative returns to the  $J/\psi$ , and  $J/\psi$  decays from the extended tail of the  $J/\psi$  Breit-Wigner distribution. It is subtracted statistically by scaling the yield of events passing the selection criteria from the off-resonance data sample. The scale factor between off- and on-resonance yields is the ratio of luminosities (measured using the process  $e^+e^- \rightarrow \gamma\gamma$  [15]) multiplied by a  $1/s$  dependence for the cross-section behavior. We subtract non-collision events statistically using an extrapolation from the tail of the  $z_{\text{vtx}}$  into the signal region. Other effects are negligible.

In a MC simulation we determine the detection efficiency for  $\psi(2S)$  decay events to be 76%. The underlying MC generator settings incorporate current branching fraction deter-

minations [11] for  $\psi(2S)$ ,  $\chi_{cJ}$ , and  $J/\psi$  decays, and for the remainder employs JETSET [16]. The agreement between data and MC simulation can be judged from Fig. 6.

To evaluate the accuracy of the estimated efficiency and background subtractions, we explore three different scenarios where we vary the requirements on track multiplicity ( $\geq 1$  to  $\geq 4$ ) with appropriate background suppression criteria modifying the aforementioned energy balances, with detection efficiencies ranging between 91% and 65%, respectively. We find a variation of 2% relative to the nominal setting, which we take as a systematic uncertainty. The largest contributors are the dependence on the trigger requirements (1.8%), followed by the tracking and energy settings (0.9%).

The procedure, when applied to a portion of the earlier-taken CLEO-c  $\psi(2S)$  data, results in a slight reduction in the result compared to the method described in Ref. [14]. This is understood to be due to updated settings of the MC generator (thereby modifying the detection efficiency), a change in the continuum background subtraction (using CLEO-c continuum data), and other improvements in the detector description.

The number of  $\psi(2S)$  decays thus determined is  $(27.36 \pm 0.57) \times 10^6$ , with a relative systematic uncertainty of 2%. The statistical uncertainty is negligible. This leads to a branching fraction  $\mathcal{B}(\psi(2S) \rightarrow \pi^+ \pi^- J/\psi) = (35.04 \pm 0.07 \pm 0.77)\%$ . This result is more precise than the one presented in Ref. [2] and also somewhat higher. This is chiefly due to an improved background and signal efficiency treatment in the inclusive  $\psi(2S)$  count.

The last column of Table I shows the absolute branching fractions, obtained by multiplying the entries in the penultimate column by  $\mathcal{B}_{+-}$  and appropriate cancellation of correlated systematic uncertainties. One independent set of numbers from the data displayed in the table is  $\mathcal{B}_{+-}$  together with the ratios to  $\mathcal{B}_{+-}$ . Some derived quantities may be computed, with the correlations properly taken into account. We find  $\mathcal{B}(\pi^0 J/\psi) / \mathcal{B}(\eta J/\psi) = (3.88 \pm 0.23 \pm 0.05)\%$ . Using  $\mathcal{B}(\psi(2S) \rightarrow \gamma \chi_{cJ}) = (9.3 \pm 0.4)\%$ ,  $(8.8 \pm 0.4)\%$ , and  $(8.1 \pm 0.4)\%$  [11] for  $J = 0, 1, 2$ , we obtain  $\mathcal{B}(\chi_{cJ} \rightarrow \gamma J/\psi) = (1.35 \pm 0.07 \pm 0.14 \pm 0.06)\%$ ,  $(40.5 \pm 0.3 \pm 1.4 \pm 1.8)\%$ ,  $(24.1 \pm 0.2 \pm 0.9 \pm 1.2)\%$ , respectively, where the first uncertainty is statistical, the second systematic from this analysis, and the third from the input branching fraction. Our result for  $\mathcal{B}(\chi_{c0} \rightarrow \gamma J/\psi)$  is considerably smaller than found in Ref. [2] and consistent with other determinations [11]. The reduction in this rate is a direct consequence of improved treatment of  $\chi_{c0}$  backgrounds.

With  $\mathcal{B}(\psi(2S) \rightarrow \gamma \chi_{cJ}, \gamma \eta_c)$  and  $\mathcal{B}(\psi(2S) \rightarrow \ell^+ \ell^-)$  ( $\ell = e, \mu, \tau$ ), our results imply [11]  $\mathcal{B}(\psi(2S) \rightarrow \text{light hadrons}) = (15.4 \pm 1.5)\%$ , or 2.9 standard deviations higher than an extrapolation arrived at by scaling  $\mathcal{B}(J/\psi \rightarrow \text{light hadrons})$  by the ratio of leptonic branching ratios,  $(12.45 \pm 0.35)\%$ . Here, all  $\psi(2S)$  results are taken from the branching fraction fit values in Ref. [11].

In summary, we have studied the exclusive decays  $\psi(2S) \rightarrow J/\psi + h$  ( $h = \pi^+ \pi^-, \pi^0 \pi^0, \eta, \pi^0$ ) and  $\psi(2S) \rightarrow \gamma \chi_{cJ} \rightarrow \gamma \gamma J/\psi$  transitions,  $J/\psi \rightarrow e^+ e^-$  and  $\mu^+ \mu^-$ , with a similar strategy applied to all channels. The analysis is complemented by a study of the inclusive mode  $\psi(2S) \rightarrow \text{any} + J/\psi$ . We have determined branching ratios between exclusive modes on the one hand and between exclusive modes and  $(\text{any} + J/\psi)$  on the other. We have also measured the branching fraction  $\psi(2S) \rightarrow \pi^+ \pi^- J/\psi$  using the dipion recoil mass spectrum, which facilitates transformation of the ratios relative to  $\pi^+ \pi^- J/\psi$  into absolute branching fractions. Further quantities are derived. The precision of all quantities given here improves upon previous measurements. The results presented here supersede those from Ref. [2].

We gratefully acknowledge the effort of the CESR staff in providing us with excellent luminosity and running conditions. This work was supported by the A.P. Sloan Foundation,

the National Science Foundation, the U.S. Department of Energy, the Natural Sciences and Engineering Research Council of Canada, and the U.K. Science and Technology Facilities Council.

---

- [1] M. B. Voloshin, arXiv:0711.4556 [hep-ph] (to appear in *Prog. Part. Nucl. Phys.*); E. Eichten *et al.*, arXiv:hep-ph/0701208 (to appear in *Rev. Mod. Phys.*).
- [2] N. E. Adam *et al.* [CLEO Collab.], *Phys. Rev. Lett.* **94**, 232002 (2005).
- [3] CLEO-c/CESR-c Taskforces & CLEO-c Collaboration, Cornell University LEPP Report No. CLNS 01/1742 (2001), unpublished.
- [4] Y. Kubota *et al.* [CLEO Collab.], *Nucl. Instrum. Methods Phys. Res., Sect. A* **320**, 66 (1992); D. Peterson *et al.*, *Nucl. Instrum. Methods Phys. Res., Sect. A* **478**, 142 (2002); M. Artuso *et al.*, *Nucl. Instrum. Methods Phys. Res., Sect. A* **502**, 91 (2003).
- [5] A. Lopez *et al.* [CLEO Collab.], *Phys. Rev. Lett.* **99**, 122001 (2007).
- [6] D.J. Lange, *Nucl. Instrum. Methods Phys. Res., Sect. A* **462**, 152 (2001).
- [7] E. Barberio and Z. Was, *Comput. Phys. Commun.* **79**, 291 (1994).
- [8] R. Brun *et al.*, GEANT 3.21, CERN Program Library Long Writeup W5013 (1993), unpublished.
- [9] J. Z. Bai *et al.* [BES Collab.], *Phys. Rev. D* **62**, 032002 (2000).
- [10] L.S. Brown and R.N. Cahn, *Phys. Rev. D* **13**, 1195 (1976).
- [11] W.-M. Yao *et al.*, *Journal of Physics, G* **33**, 1 (2006) and 2007 partial update for 2008.
- [12] J. D. Jackson, “Lectures On The New Particles,” proceedings of the SLAC summer institute, August 1976, <http://www.slac.stanford.edu/pubs/confproc/ssi76/ssi76-005.html>.
- [13] Z. Li *et al.* [CLEO Collab.], *Phys. Rev. D* **71**, 111103 (2005).
- [14] S. B. Athar *et al.* [CLEO Collab.], *Phys. Rev. D* **70**, 112002 (2004).
- [15] S. Dobbs *et al.* [CLEO Collab.], *Phys. Rev. D* **76**, 112001 (2007).
- [16] T. Sjöstrand *et al.*, *Computer Physics Commun.* **135**, 238 (2001).

TABLE I: For each channel: the number of events observed in  $J/\psi \rightarrow \mu^+\mu^-$  after background subtraction and the detection efficiency ratio  $r_h^\mu \equiv \epsilon(\psi(2S) \rightarrow h + J/\psi\mu^+\mu^-)/\epsilon(\psi(2S) \rightarrow \text{any} + J/\psi\mu^+\mu^-)$ ; the same for  $J/\psi \rightarrow e^+e^-$ ; the ratio of branching fractions  $\mathcal{B}(\psi(2S) \rightarrow h + J/\psi)$  and  $\mathcal{B}(\psi(2S) \rightarrow \text{any} + J/\psi)$ ; the same with respect to  $\mathcal{B}_{+-}$ ; absolute branching fractions.

Channels	$N^\mu$	$r_h^\mu$	$N^e$	$r_h^e$	$\mathcal{B}/\mathcal{B}_{\text{any}} \text{ (%)}$	$\mathcal{B}/\mathcal{B}_{+-} \text{ (%)}$	$\mathcal{B} \text{ (%)}$
$\pi^+\pi^- J/\psi$	302030	0.80	263372	1.01	$56.04 \pm 0.09 \pm 0.62$	$\equiv 100$	$35.04 \pm 0.07 \pm 0.77$
$\pi^0\pi^0 J/\psi$	32249	0.17	28746	0.22	$28.29 \pm 0.12 \pm 0.56$	$50.47 \pm 0.22 \pm 1.02$	$17.69 \pm 0.08 \pm 0.53$
$\eta J/\psi$	9819	0.27	8590	0.33	$5.49 \pm 0.06 \pm 0.09$	$9.79 \pm 0.10 \pm 0.15$	$3.43 \pm 0.04 \pm 0.09$
$\pi^0 J/\psi$	289	0.19	238	0.25	$0.213 \pm 0.012 \pm 0.003$	$0.380 \pm 0.022 \pm 0.005$	$0.133 \pm 0.008 \pm 0.003$
$\gamma(\gamma J/\psi)_{\chi_{c0}}$	308	0.22	253	0.28	$0.201 \pm 0.011 \pm 0.021$	$0.358 \pm 0.020 \pm 0.037$	$0.125 \pm 0.007 \pm 0.013$
$\gamma(\gamma J/\psi)_{\chi_{c1}}$	13244	0.34	11619	0.44	$5.70 \pm 0.04 \pm 0.15$	$10.17 \pm 0.07 \pm 0.27$	$3.56 \pm 0.03 \pm 0.12$
$\gamma(\gamma J/\psi)_{\chi_{c2}}$	6616	0.31	5768	0.40	$3.12 \pm 0.03 \pm 0.09$	$5.56 \pm 0.05 \pm 0.16$	$1.95 \pm 0.02 \pm 0.07$
any + $J/\psi$	676889	$\equiv 1$	466153	$\equiv 1$	$\equiv 100$	$178.4 \pm 0.3 \pm 2.0$	$62.54 \pm 0.16 \pm 1.55$

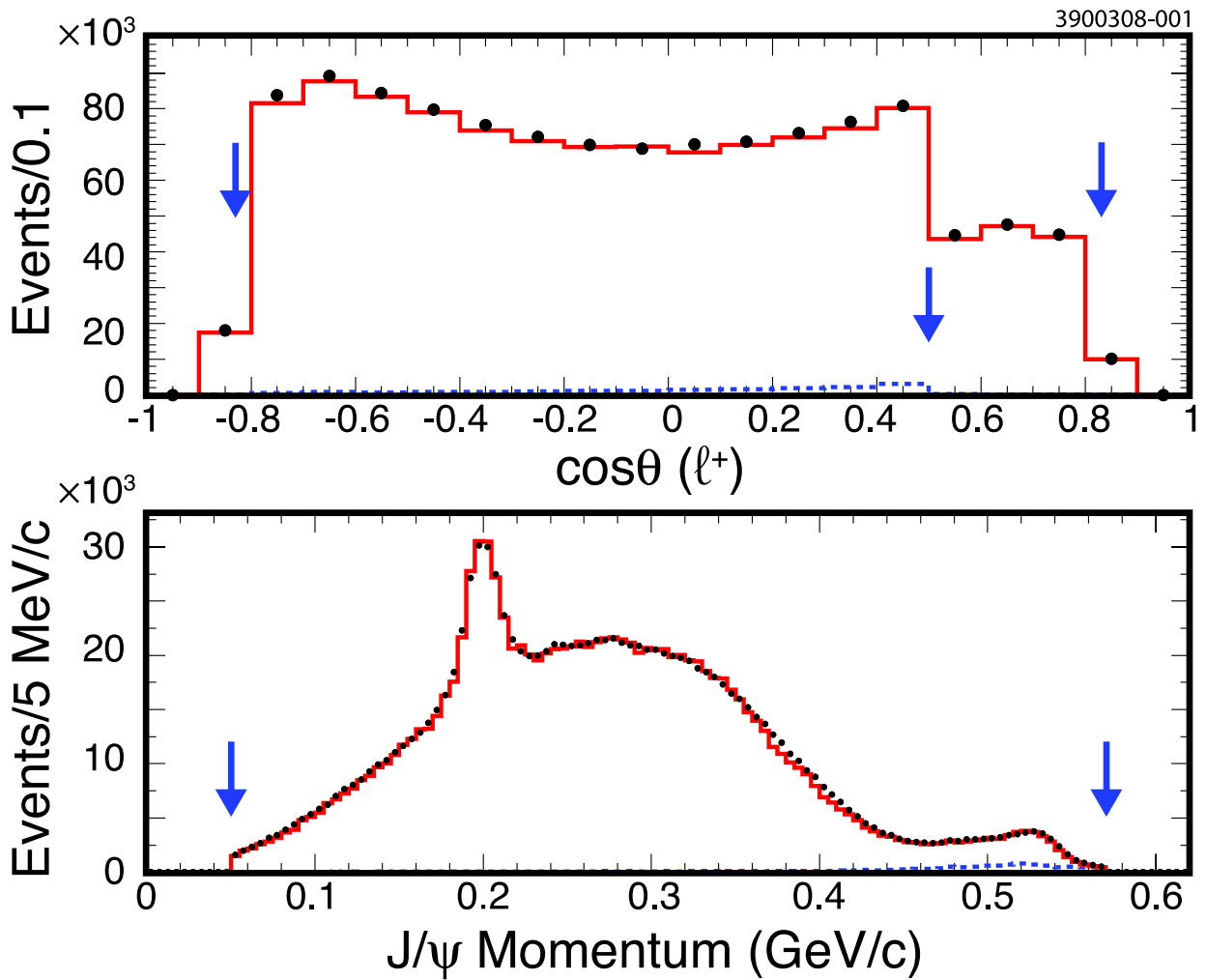


FIG. 1: Distributions relevant to any  $+ J/\psi$ . Top: polar angle of the positive lepton. For  $e^+e^-$  only, we demand  $\cos\theta_{e^+} < 0.5$  to suppress Bhabha events with initial/final state radiation or bremsstrahlung in detector material. Bottom:  $J/\psi$  momentum. Solid circles show the on- $\psi(2S)$  data, dashed histogram the continuum data (scaled by luminosity and  $1/s$ ) taken at  $E_{\text{cm}} = 3.67$  GeV, the solid histogram represents the sum of all MC exclusive channels (scaled to match the data in signal modes). Arrows appear at nominal selection values.

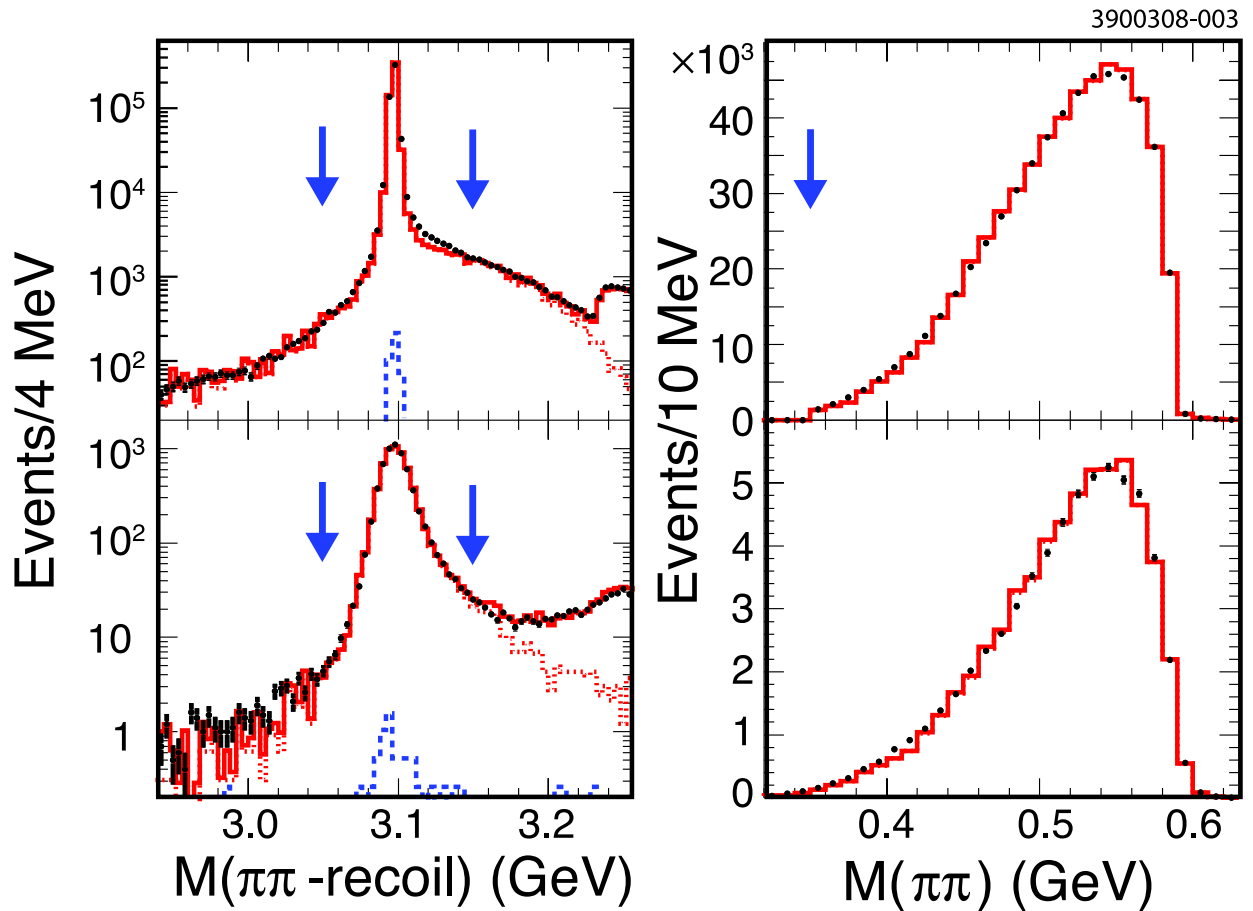


FIG. 2: Plots relevant to the decay  $\psi(2S) \rightarrow \pi^+\pi^-J/\psi$  (top) and  $\psi(2S) \rightarrow \pi^0\pi^0J/\psi$  (bottom). The left plots show the dipion recoil mass spectrum and the right plots the dipion mass spectrum. The  $J/\psi$  candidates in the continuum sample arise from the tail of the  $\psi(2S)$ . Symbols are as in Fig. 1. The dotted line represents the simulated signal.

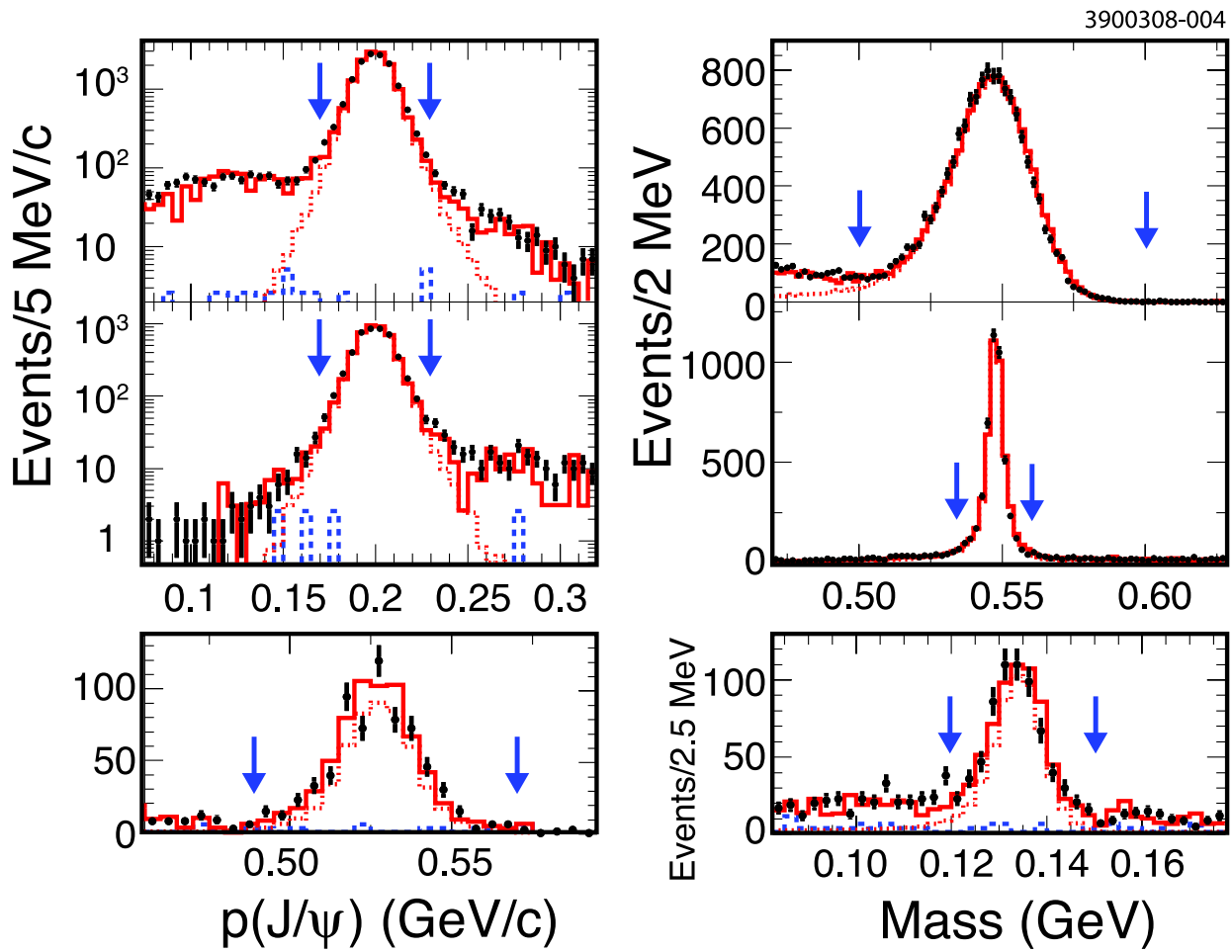


FIG. 3:  $\psi(2S) \rightarrow \eta J/\psi$ ,  $\eta \rightarrow \gamma\gamma$  (top) and  $\eta \rightarrow \pi^+\pi^-\pi^0$  (middle), and  $\psi(2S) \rightarrow \pi^0 J/\psi$  (bottom): The  $J/\psi$  momentum (left) and invariant mass of the decay products (right). Symbols are as in Fig. 1. The dotted line represents the simulated signal.

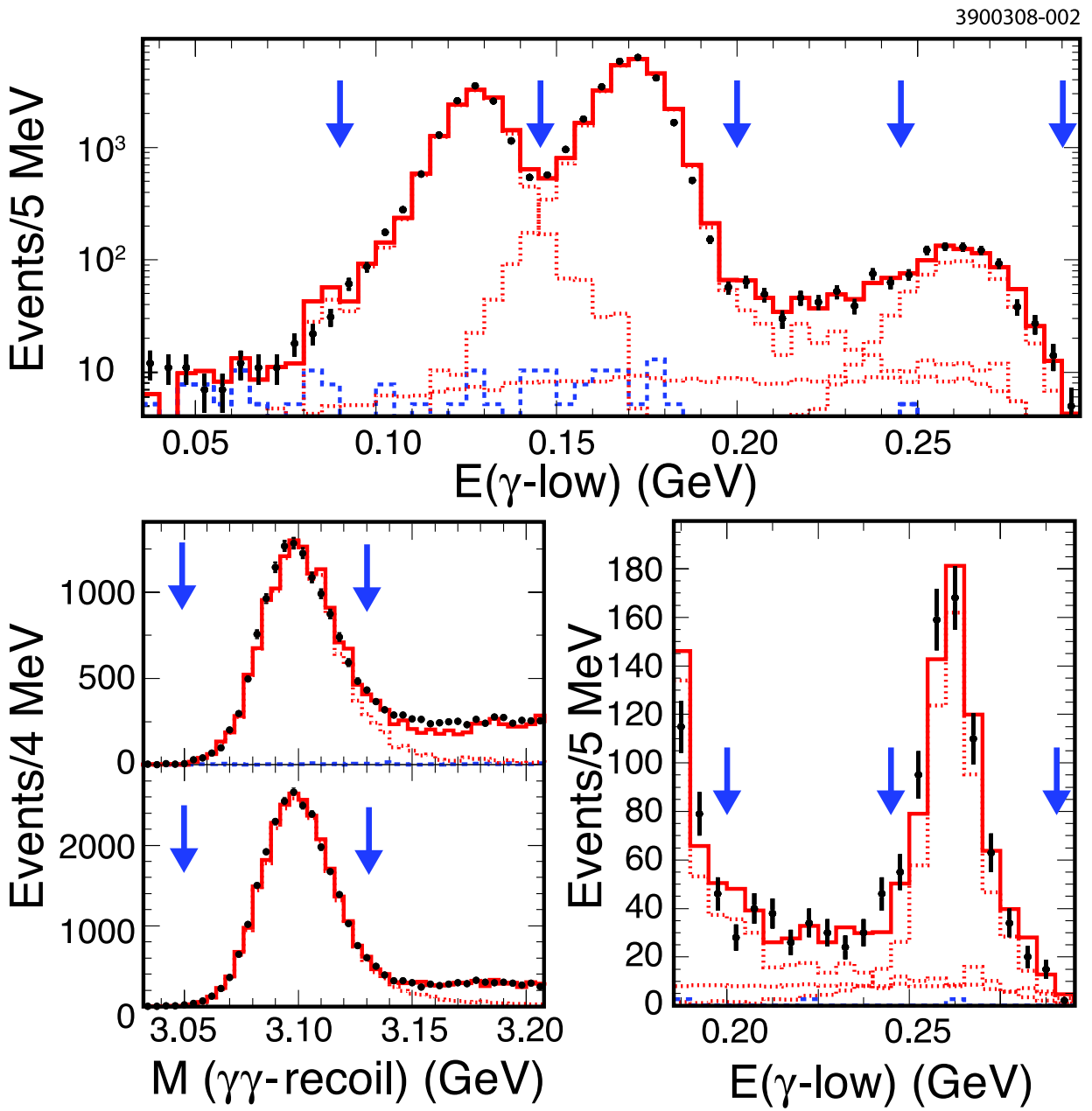


FIG. 4: For the decays  $\psi(2S) \rightarrow \gamma\gamma J/\psi$ ,  $E_{\gamma\text{-low}}$  (top) before applying the full-event kinematic fit to the area above  $E_{\gamma\text{-low}} = 200$  MeV, the di-photon recoil mass for  $\chi_{c2,1}$  (middle [lower] left for  $J = 2$  [ $J = 1$ ]), and  $E_{\gamma\text{-low}}$  after the full-event kinematic fit (lower right). Symbols are as in Fig. 1. The dotted line represents the simulated signal.

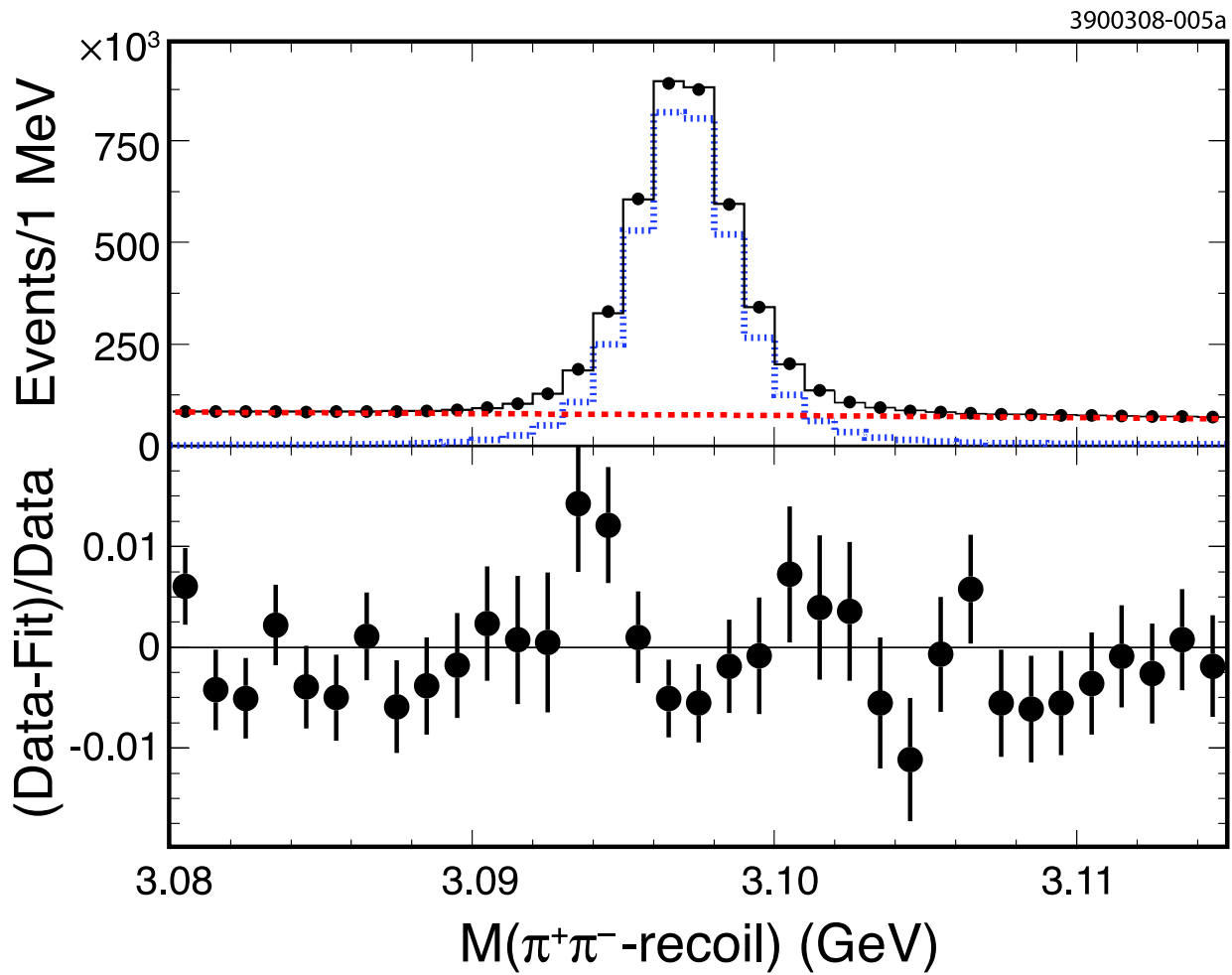


FIG. 5: The dipion recoil mass spectrum for  $\pi^+\pi^- J/\psi$ ,  $J/\psi \rightarrow X$ . Top: data points (black) overlaid with the fit result (solid black curve) obtained using a (scaled) signal shape from  $\pi^+\pi^- J/\psi$ ,  $J/\psi \rightarrow \ell^+\ell^-$ , and a second-order polynomial background shape (red dashed curve). Bottom: the fractional difference between the fit and the data.

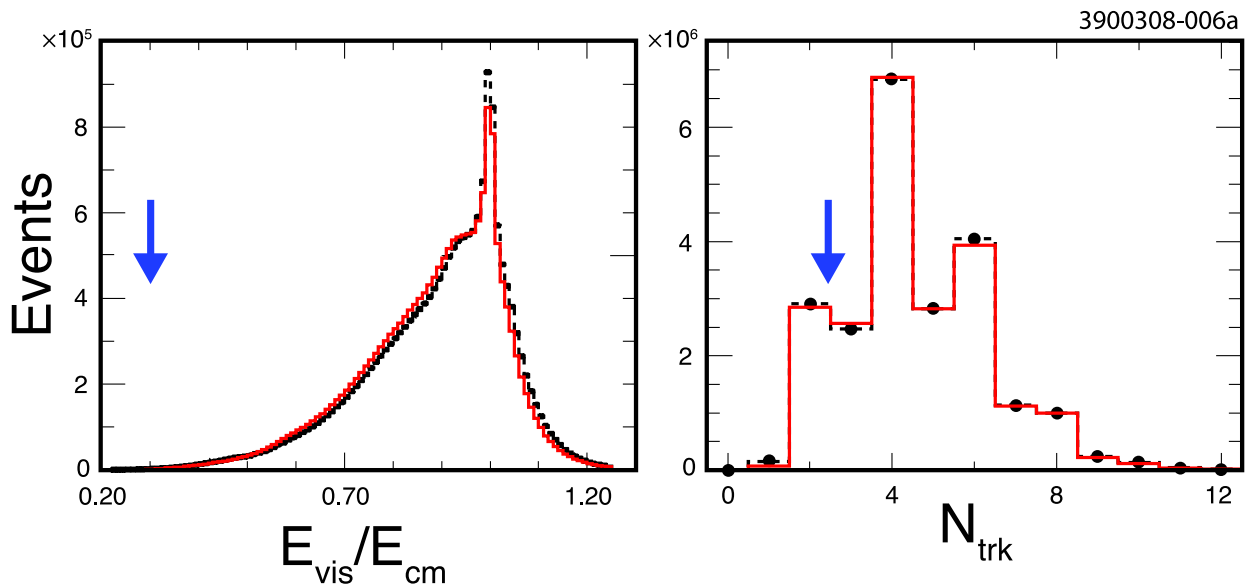


FIG. 6: Scaled energy in the event  $E_{\text{vis}}$  (left) and number of tracks (right), for data (dashed black line / points) and simulation (solid red line). The right distribution has been obtained with the selection based on  $N_{\text{trk}} \geq 1$ .